Sodium borohydride as an n-type dopant in tris(8-hydroxyquinoline) aluminium thin film

You may also be interested in:

Highly power efficient organic light-emitting diodes
Junwei Ma, X Y Jiang, Zhang Liang et al.

Organic light-emitting diodes based on p- and n-doped layers
M A Khan, Wei Xu, Khizar-ul-Haq et al.

ReOx charge injection/blocking layers in organic electronic devices
Jiaxiu Luo, Lixin Xiao, Zhijian Chen et al.

Improved electron injection in organic light-emitting devices with a lithium acetylacetonate
[Li(acac)]/aluminium bilayer cathode
Shengwei Shi, Dongge Ma and Junbiao Peng

An effective electron injection material to realize high-efficiency I-TOLEDs
Qiang Wang, Fengxia Wang, Xianfeng Qiao et al.

A pentacene-doped hole injection layer for organic light-emitting diodes
Shengwei Shi and Dongge Ma

Effect of NaCl doped into Bphen layer on the performance of tandem organic light-emitting diodes
Xiao Zhi-Hui, Wu Xiao-Ming, Hua Yu-Lin et al.

Tandem organic light-emitting diode with a molybdenum tri-oxide thin film interconnector layer
Lu Fei-Ping, Wang Qian and Zhou Xiang

Influence of p-doping hole transport layer on the performance of organic light-emitting devices
M A Khan, Wei Xu, Khizar-ul-Haq et al.

Sodium borohydride as an n-type dopant in tris(8-hydroxyquinoline) aluminium thin film

Bo Jiao, Zhaoxin Wu[1], Yang Dai, Dongdong Wang and Xun Hou

Key Laboratory for Physical Electronics and Devices of the Ministry of Education, School of Electronic
and Information Engineering, Xi'an Jiaotong University, Xi'an, Shaanxi 710049,
People's Republic of China

E-mail: zhaoxinwu@mail.xjtu.edu.cn

Abstract
An efficient n-type dopant, sodium borohydride ($NaBH_4$), in tris(8-hydroxyquinoline)
aluminium (Alq_3) thin film has been developed. Doping $NaBH_4$ in Alq_3 can significantly
enhance the electron injection and transport, which can reduce the applied voltage and
improve the efficiency of organic light-emitting diodes compared with the referenced device.
Using the quartz crystal microbalance test, we demonstrated that $NaBH_4$ decomposes
following gas formation during the thermal evaporation process. By calculating the deposited
fraction of $NaBH_4$, we concluded that boron and metallic sodium were the main components
of the dopant, while gaseous hydrogen formed during the evaporation process. We thus found
that, among these two components, metallic sodium is most likely to be the active component
of the dopant because of its strong electron donor characteristic.

(Some figures in this article are in colour only in the electronic version)

1. Introduction

Recently, based on different kinds of organic semi-conductor materials, significant progress has been made in realizing efficient organic devices such as organic light-emitting diodes (OLEDs) [1–4], organic thin-film field-effect transistors (OTFTs) [5–7] and organic photovoltaic cells [8–11]. Compared with the traditional inorganic semiconductor materials, organic semiconductor materials exhibit some remarkable advantages, such as their potential for low-cost fabrication and large variation of organic chemical structures. However, their carrier concentration and carrier mobility are rather low. Therefore, the optimizations of charge injection and carrier transport play a crucial role in the design of organic electronic and optoelectronic devices.

Electrical doping is an efficient approach for enhancing carrier injection and transport in organic semiconductors, which is similar to inorganic semiconductors. For p-type doping, F_4-TCNQ [12–14], a strong electron acceptor, is considered as an ideal p-type dopant which

is extensively used in a variety of materials, such as N, N'-biphenyl-N, N'-bis(1-naphthyl)-(1,1'-biphenyl)-4,4'-diamine (NPB) [13], 4,4',4''-tris[N-(3-methylphenyl)-N-phenylamino] triphenylamine (m-MTDATA) [15], and zinc phthalocyanine (ZnPc) [16]. For n-type doping, the n-type dopants widely used are alkaline metals, such as lithium and caesium [17–19]. However, special equipment is needed to handle those dopants because of their acute reactivity, which is particularly problematic. Thus it is still desirable to find stable and efficient n-type dopants. In this work, sodium borohydride ($NaBH_4$) was demonstrated to be an efficient n-type doping material in tris(8-hydroxyquinoline) aluminium (Alq_3) thin film. The thermal stability of $NaBH_4$ during the evaporation process was investigated by the quartz crystal microbalance (QCM) method. By calculating the deposited fraction of $NaBH_4$, we conclude that boron and metallic sodium are the main components of the dopant, in which the metallic sodium was supposed to be the active component because of its strong electron donor characteristic. Since $NaBH_4$ is a cheap and widely used reducing agent, this technology will be beneficial for the development of low-cost organic electronic devices.

[1] Author to whom any correspondence should be addressed.

2. Experiments

In our experiments, n-type doping in Alq_3 was realized by the co-evaporation of $NaBH_4$ and Alq_3. All the devices were fabricated and measured in the way described in [20]. A series of electron-only devices were fabricated to investigate the electron injection and transport characteristics with a structure of indium tin oxide (ITO)/n-doped Alq_3 layer (100 nm)/Al (100 nm). In devices A, B, C and D, the doping concentrations of $NaBH_4$ in Alq_3 were 0%, 0.5%, 2% and 5% in volume ratio, respectively. In addition, an undoped device E with a LiF/Al cathode, which is widely used to improve the electron injection in OLEDs, was also fabricated as a reference device. The configuration of device E is ITO/Alq_3 (100 nm)/LiF (0.5 nm)/Al (100 nm). Both device structures are depicted in figure 1(*a*). Current density–voltage–luminance (J–V–L) characteristics were measured using a computer-controlled sourcemeter (Keithley 2602) and a calibrated silicon photodiode. All the measurements were carried out at room temperature under ambient conditions. The device used for the QCM test was a regular quartz crystal thickness monitor, which was placed approximately 22 cm above the evaporation boat (a home-made molybdenum boat), and was water cooled to lower the surface temperature. The temperature of the evaporation boat was controlled by adjusting the source current I of the power supply, which was increased by 5 A every 3 min to prevent the material from spattering during evaporation.

3. Results and discussion

Current density–voltage (J–V) characteristics of the electron-only devices were measured to investigate the doping effect of $NaBH_4$ in Alq_3 by sweeping the voltage from −10 to 10 V. Figure 1(*b*) shows the J–V characteristics of the electron-only devices. When the voltage was swept from −10 to 0 V, the ITO electrode acted as the cathode and the Al electrode as the anode, while the ITO acted as the anode and Al as the cathode when the voltage was swept from 0 to 10 V. No matter which electrode acts as the cathode, the ITO electrode for the negative voltage region and the Al electrode for the positive voltage region, all the $NaBH_4$-doped devices, B, C and D, exhibit better performance than the undoped device A and device E, as shown in figure 1(*b*). This result indicates that $NaBH_4$ doping in Alq_3 can significantly improve the ability of electron injection and transport. The J–V characteristics of the electron-only devices were zoomed in for detailed depiction, as shown in the inset of figure 1(*b*). It is clear that device C (doped with 2% $NaBH_4$) shows the highest current density among the five devices at the same applied voltage. For example, at the applied voltage of 10 V, the current densities of the undoped device A and device E with the LiF/Al composite cathode are 1 A m^{-2} and 430 A m^{-2}, respectively. For device B (doped with 0.5% $NaBH_4$) and device D (doped with 5% $NaBH_4$), the current densities are 870 A m^{-2} and 350 A m^{-2}, respectively, and for the optimally doped device C (doped with 2% $NaBH_4$), the current density reaches 4100 A m^{-2} at this applied voltage.

To further demonstrate the n-type doping effect of $NaBH_4$ in Alq_3, three OLEDs were fabricated with structures
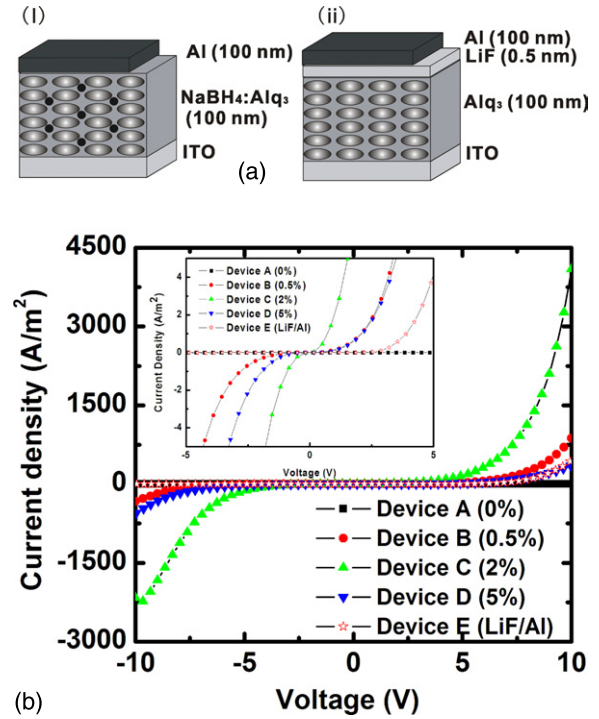
Figure 1. (*a*) Configuration of the electron-only devices: (i) $NaBH_4$ doped Alq_3 device (devices A, B, C and D); (ii) Alq_3 device with LiF/Al composite cathode (device E). (*b*) Current density–voltage (J–V) characteristics for $NaBH_4$ doped Alq_3 devices (devices A–D). Data for a device with LiF/Al composite cathode (device E) is also shown. Inset shows the zoom-in of the same data in the low-current and low-voltage region.

of ITO/NPB (60 nm)/Alq_3 (60 nm)/Al (100 nm) (device F), ITO/NPB (60 nm)/Alq_3 (60 nm)/LiF (0.5 nm)/Al (100 nm) (device G) and ITO/NPB (60 nm)/Alq_3 (40 nm)/Alq_3 : 2% $NaBH_4$ (20 nm)/Al (100 nm) (device H). The configurations of the three devices are shown in figure 2(*a*). The J–V and L–V curves of devices F–H are shown in figure 2(*b*), and the characteristics of the current efficiency and power efficiency as a function of the luminance are shown in figure 2(*c*). Among the three devices, device H with 2% $NaBH_4$ doped electron-transport layer exhibits the lowest voltage at the same current density, which means doping of $NaBH_4$ can efficiently reduce the driving voltage of OLEDs, as shown in figure 2(*b*). As shown in figure 2(*c*), device H shows higher power efficiency and current efficiency compared with devices F and G. For example, at 1000 cd m^{-2}, the power efficiency of device F is 1.7 lm W^{-1} (3.5 cd A^{-1} at 6.4 V), which is 42% higher than that of device G at 1000 cd m^{-2} (1.2 lm W^{-1} and 2.8 cd A^{-1} at 7.4 V) and 240% higher than that of device F at 1000 cd m^{-2} (0.5 lm W^{-1} and 1.8 cd A^{-1} at 10.8 V). Those data clearly demonstrate that the electron injection is further enhanced by doping $NaBH_4$ into Alq_3 compared with the conventional LiF/Al cathode. As we know, holes are the major carriers and electrons are the minor carriers [21] in typical bi-layer OLEDs (e.g. device F). One typical method to improve the balance of holes and electrons is to reduce the transport of holes by, e.g., doping rubrene into the hole-transporting layer [22] or doping hole-blocking material, such as bathocuproine (BCP) [23], in Alq_3. This method, however, will increase the turn-on voltage
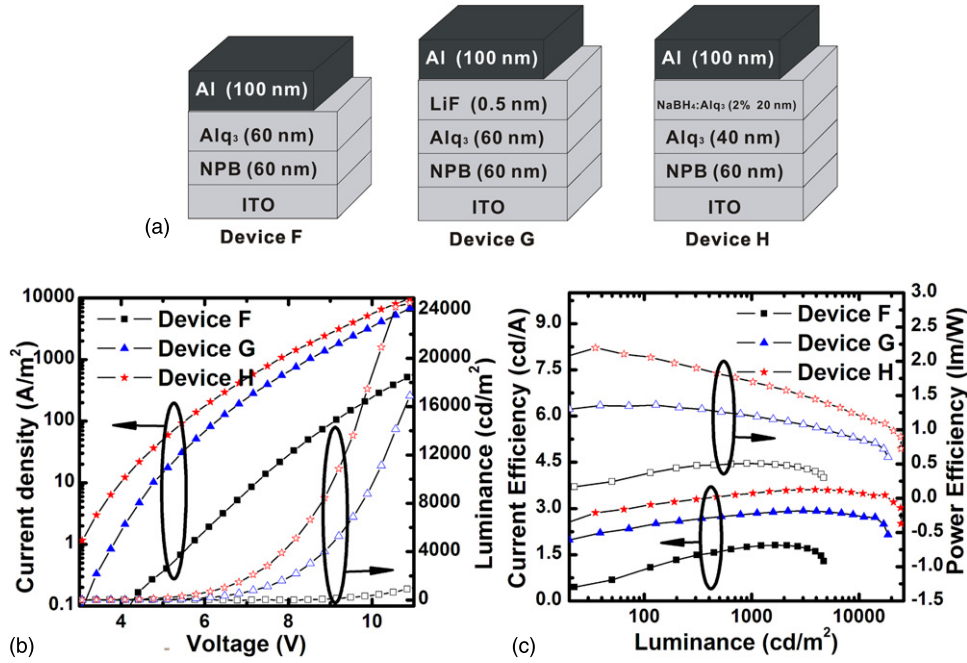
Figure 2. (*a*) Configurations of devices F, G and H. (*b*) The current density–voltage (*J*−*V*) and luminance–voltage (*L*−*V*) curves of devices F, G and H. (*c*) Current efficiency–luminance and power efficiency–luminance characteristics of devices F, G and H.

of the OLEDs, while increasing its efficiency. An alternative method is to enhance electron injection and transport, such as n-type doping NaBH$_4$ in Alq$_3$, just as demonstrated in the above study of doped electron-only devices. As shown in figures 2(*b*) and (*c*), the n-type doping of NaBH$_4$ in Alq$_3$ can not only improve the balance between holes and electrons in OLEDs but also reduce the applied voltage of OLEDs, which is important in the practical application of OLEDs.

The QCM test [24–27] was used to evaluate the thermal stability of NaBH$_4$ during the evaporation process. For a thermally stable material, it is believed that the frequency shift of the QCM (ΔF_S) would be proportional to the mass loss of the boat (ΔM) [26]:

$$\Delta F_S = K \Delta M, \qquad (1)$$

where K is a positive constant which is independent of the materials used. While for a material which is thermally unstable, only a fraction ($d\%$) of the mass loss of the boat was deposited during the evaporation, so the frequency shift of the QCM for unstable material (ΔF_{NS}) is given by

$$\Delta F_{NS} = (d\%) K \Delta M. \qquad (2)$$

If the mass of the stable and unstable materials that are loaded in the boat are the same, according to equations (1) and (2), the deposited fraction ($d\%$) of the unstable material can be obtained from equation (3):

$$d\% = \Delta F_{NS} / \Delta F_S. \qquad (3)$$

In our experiments, NPB, m-MTDATA, LiF and NaBH$_4$ are used for the QCM test. Among these four materials, NPB, m-MTDATA and LiF are known to be stable during evaporation and are used as in [1, 26]. Figure 3 shows
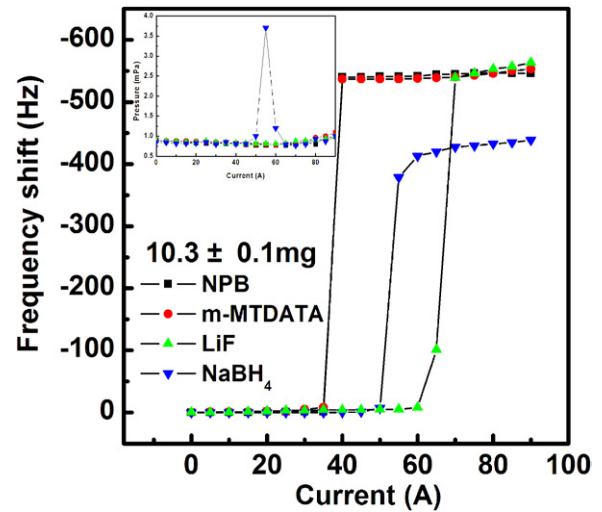

Figure 3. Frequency shift–source current (ΔF−I) curves of NPB, m-MTDATA, LiF and NaBH4, respectively, at same amounts of source materials (10 mg). Inset is the change in pressure in vacuum chamber with the increase in source current during the evaporation of NPB, m-MTDATA, LiF and NaBH4, respectively.

frequency shift–source current (ΔF−I) curves of NPB, m-MTDATA, LiF and NaBH$_4$ with the same source mass of 10 mg, respectively. The residual mass after evaporation was less than 1% of the initial amount (10 mg) for NaBH$_4$, while almost no residue was observed for the other materials. As shown in figure 3, it is found that the frequency shifts of NPB, m-MTDATA and LiF are almost identical when experimental errors are considered, while NaBH$_4$ exhibits a much lower shift in frequency than the other materials. From the inset in figure 3, we found that the pressure in the vacuum chamber changed dramatically during the thermal

Table 1. Measured frequency shift (ΔF) and the corresponding deposited fraction ($d\%$). The evaporated weights of all the samples are kept at the same value of 10 mg.

Materials	Frequency shift (ΔF) (Hz)	Deposited fraction (d%) $\Delta F/\Delta F$(NPB)(%)
NPB	-544 ± 15	—
m-MTDATA	-537 ± 11	99 ± 2
LiF	-563 ± 9	104 ± 2
$NaBH_4$	-439 ± 16	81 ± 3

evaporation of $NaBH_4$, which is in contrast to the evaporation of the other three materials. These phenomena indicate the thermal decomposition of $NaBH_4$ and the formation of gas. The deposited fraction ($d\%$) of m-MTDATA, LiF and $NaBH_4$ are calculated and shown in table 1 using NPB as a standard material. The deposited fractions of m-MTDATA and LiF are around 100%, indicating they are thermally stable materials. However, the deposited fraction of $NaBH_4$ is $(81 \pm 3)\%$, much less than 100%, which indicates that the decomposition of $NaBH_4$ occurs during evaporation. Ostroff *et al* have reported that $NaBH_4$ will decompose around 400 °C in vacuum according to the following reaction [28, 29]:

$$NaBH_4 + heat \xrightarrow{\text{vacuum}} Na + B + 2H_2. \qquad (4)$$
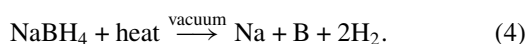
According to this reaction, the theoretical deposited fraction (the ratio of the sum of molecular weight of Na and B to that of the $NaBH_4$) of $NaBH_4$ should be 89.4%, which is slightly larger than our experimental value ($(81 \pm 3)\%$). The reason for this minor difference is still under investigation. A possible explanation is that gaseous diborane (B_2H_6) may form during the evaporation, which will decrease the deposition of boron. Therefore, we conclude that the main components of dopant are boron and metallic sodium based on the QCM test and the report of Ostroff *et al*. Metallic sodium has been used as an n-dopant in naphthalene tetracarboxylic anhydride (NTCDA) because of its strong electron donor characteristic (ionization potential $= 5.14$ eV) [30]. Boron, however, is unlikely to act as an electron donor due to its higher ionization potential, 8.29 eV. So metallic sodium should be the active component of the dopant. These results also help us to understand the dependence of the $J–V$ characteristic of the doped Alq_3 film on the doping concentration of the $NaBH_4$, as shown in figure 1(*b*). The current density at all applied voltages increases with $NaBH_4$ doping because of the existence of the metallic sodium. The optimum doping concentration of $NaBH_4$ is around 2%. Beyond 2% concentration, the decrease in the current density with doping concentration might be due to the aggregation of boron. A thorough explanation requires experimental investigation of the effect of doping boron in Alq_3, which has not been reported in the literature and is still under investigation.

4. Conclusion

In summary, we have demonstrated an efficient n-dopant, $NaBH_4$, that was used in doping Alq_3 film. Doping $NaBH_4$ in

Alq_3 can significantly increase the electron current density and electron injection. This doping technology can further reduce the applied voltage and improve the efficiency of the OLEDs because of the enhanced electron injection and transport. The thermal evaporation process of $NaBH_4$ has been investigated using the QCM method. By calculating the deposited fraction of $NaBH_4$, it is concluded that the main components of the dopant are boron and metallic sodium, while the metallic sodium is the active component of the dopant because of its strong electron donor characteristic. Our technology will be beneficial for the development of low-cost organic electronic devices because $NaBH_4$ is an inexpensive material and its processing is much safer than that of alkaline metals.

References

[1] Hung L S and Chen C H 2002 *Mater. Sci. Eng.* R **39** 143(Reports)
[2] Tang C W and Vanslyke S A 1987 *Appl. Phys. Lett.* **51** 913
[3] Sheats J R, Antoniadis H, Hueschen M, Leonard W, Miller J, Moon R, Roitman D and Stocking A 1996 *Science* **273** 884
[4] He G F, Pfeiffer M, Leo K, Hofmann M, Birnstock J, Pudzich R and Salbeck J 2004 *Appl. Phys. Lett.* **85** 3911
[5] Garnier F, Hajlaoui R, Yassar A and Srivastava P 1994 *Science* **265** 1684
[6] Dimitrakopoulos C D, Purushothaman S, Kymissis J, Callegari A and Shaw J M 1999 *Science* **283** 822
[7] Katz H E 2004 *Chem. Mater.* **16** 4748
[8] Peumans P, Yakimov A and Forrest S R 2003 *J. Appl. Phys.* **93** 3693
[9] Hoppe H and Sariciftci N S 2004 *J. Mater. Res.* **19** 1924
[10] Rand B P, Genoe J, Heremans P and Poortmans J 2007 *Prog. Photovolt.* **15** 659
[11] Gunes S, Neugebauer H and Sariciftci N S 2007 *Chem. Rev.* **107** 1324
[12] Gao W Y and Kahn A 2001 *Appl. Phys. Lett.* **79** 4040
[13] Gao W Y and Kahn A 2003 *J. Appl. Phys.* **94** 359
[14] Hwang J and Kahn A 2005 *J. Appl. Phys.* **97** 103705
[15] Huang J S, Pfeiffer M, Werner A, Blochwitz J, Leo K and Liu S Y 2002 *Appl. Phys. Lett.* **80** 139
[16] Blochwitz J, Fritz T, Pfeiffer M, Leo K, Alloway D M, Lee P A and Armstrong N R 2001 *Org. Electron.* **2** 97
[17] Kido J and Matsumoto T 1998 *Appl. Phys. Lett.* **73** 2866
[18] Parthasarathy G, Shen C, Kahn A and Forrest S R 2001 *J. Appl. Phys.* **89** 4986
[19] Ding H J and Gao Y L 2008 *Appl. Phys. Lett.* **92** 053309
[20] Wu Z, Jiao B, Zhao X, Hou X, Wang L, Wang H, Gao Y and Qiu Y 2009 *Thin Solid Films* **517** 3382
[21] Aziz H, Popovic Z D, Hu N X, Hor A M and Xu G 1999 *Science* **283** 1900
[22] Aziz H and Popovic Z D 2002 *Appl. Phys. Lett.* **80** 2180
[23] Wu Z J, Yang H S, Duan Y, Xie W F, Liu S Y and Zhao Y 2003 *Semicond. Sci. Technol.* **18** L49
[24] Buttry D A and Ward M D 1992 *Chem. Rev.* **92** 1355

J. Phys. D: Appl. Phys. **42** (2009) 205108

B Jiao *et al*

[25] Ganzorig C and Fujihira M 2004 *Appl. Phys. Lett.* **85** 4774

[26] Li Y, Zhang D Q, Duan L, Zhang R, Wang L D and Qiu Y 2007 *Appl. Phys. Lett.* **90** 012119

[27] Hu J M, Liu L J, Danielsson B, Zhou X D and Wang L L 2000 *Anal. Chim. Acta* **423** 215

[28] Ostroff A G and Sanderson R T 1957 *J. Inorg. Nucl. Chem.* **4** 230

[29] Drozd V, Saxena S, Garimella S V and Durygin A 2007 *Int. J. Hydrogen Energy* **32** 3370

[30] Suemori K, Yokoyama M and Hiramoto M 2005 *Appl. Phys. Lett.* **86** 173505